DOI: https://doi.org/10.24425/amm.2025.156261

M.S. ABDUL AZIZ©¹, C.Y. KHOR©²*, M.R.M. SABRI¹, R. KAMARUDIN©¹, W. RAHIMAN©³, D.S. CHE HALIN©⁴,5, P. PIETRUSIEWICZ©⁶

INFLUENCE OF TEMPERATURE ON FLEXIBLE PRINTED CIRCUIT BOARD DURING REFLOW SOLDERING

The increasing demand for flexible, lightweight, compact, and cost-effective electronic products has led to a growing preference for Flexible Printed Circuit Boards over Rigid Printed Circuit Boards. However, thermal challenges during the reflow soldering process can significantly impact FPCBs. When exposed to elevated temperatures, Flexible Printed Circuit Boards are highly susceptible to deflection and thermal stress. This study examines the impact of temperature profile on FPCBs during the reflow soldering. Deformation measurements for both FPCBs and Rigid Printed Circuit Boards were obtained using a KEYENCE LK-G152 laser sensor installed at a reflow oven's entry and exit points. The experiment evaluated two temperature profiles, soaking and ramp profile, as variables. Findings revealed that FPCBs experienced greater deformation under the ramp profile, whereas RPCBs exhibited more deformation under the soaking profile. This research provides valuable insights for engineers and Printed Circuit Board designers, offering practical guidelines for optimizing mass production in the microelectronics industry.

Keywords: Flexible Printed Circuit Boards; Rigid Printed Circuit Boards; Temperature profile; reflow soldering; deformation

1. Introduction

Flexible Printed Circuit Boards (FPCBs), which have a complete set of advantages such as being thinner, more flexible, and less expensive than Rigid Printed Circuit Boards (RPCBs), are widely used as an alternative to the RPCB. Due to their lower thickness than RPCBs, FPCBs are lightweight and flexible, which have attracted considerable attention in research and development [1,2]. FPCBs have been used in various industries. They are employed to mount flow sensors for heat and flow detection and as flexible wet sensor sheets to detect diaper urination. These sensors are more sensitive than made on RPCBs [3,4]. FPCB antennas, especially Samsung Electronics' Galaxy S6, became the main option of the electronics industry as its antenna performance surpassed Laser Direct Structuring (LDS) antennas. FPCB antennas do not need ferrite sheets for electromagnetic shielding, unlike LDS antennas, which suffer from electromagnetic interference in metal and confined environments; they are lightweight and sticker-like. They are also smaller, cheaper, and high-performance [5]. FPCBs have also been investigated in personal computer motherboards, where durability and long-term performance are paramount [6]. Flexible PCBs have emerged as a hot research area to address the increasing need for flexible and printable devices.

Reflow soldering is employed during the assembly process of FPCBs to solder the surface-mount components and devices. Reflow soldering is an essential step in the surface-mount technology (SMT) production line, which is a technology used for the permanent joining of surface-mount devices to Printed Circuit Boards (PCBs) [7]. Generally, three primary methods are used to attach SMCs to PCBs: wave soldering, reflow soldering, and conductive adhesive curing. Of these processes, reflow soldering is preferred for its yield and reliability. The few main steps of the SMT production line include solder paste printing, component placement, and the reflow soldering process [8]. The most common method for this step is solder paste printing, in which

^{*} Corresponding author: cykhor@unimap.edu.my



UNIVERSITI SAINS MALAYSIA, SCHOOL OF MECHANICAL ENGINEERING, 14300 NIBONG TEBAL, SEBERANG PERAI SELATAN, PENANG, MALAYSIA

UNIVERSITI MALAYSIA PERLIS (UNIMAP), FACULTY OF MECHANICAL ENGINEERING & TECHNOLOGY, 02600 ARAU, PERLIS, MALAYSIA.
 UNIVERSITI SAINS MALAYSIA, SCHOOL OF ELECTRICAL AND ELECTRONIC ENGINEERING, 14300 NIBONG TEBAL, SEBERANG PERAI SELATAN, PENANG, MALAYSIA.

⁴ UNIVERSITI MALAYSIA PERLIS (UNIMAP), FACULTY OF CHEMICAL ENGINEERING & TECHNOLOGY KOMPLEKS PUSAT PENGAJIAN JEJAWI 2, TAMAN MUHIBBAH, 02600, ARAU, PERLIS, MALAYSIA

⁵ UNIVERSITI MALAYSIA PERLIS (UNIMAP), CENTRE OF EXCELLENT GEOPOLYMER AND GREEN TECHNOLOGY (CEGEOGTECH), KOMPLEKS PUSAT PENGAJIAN JEJAWI 2, TA-MAN MUHIBBAH, 02600, ARAU, PERLIS, MALAYSIA

⁶² CZESTOCHOWA UNIVERSITY OF TECHNOLOGY, FACULTY OF PRODUCTION ENGINEERING AND MATERIALS TECHNOLOGY, DEPARTMENT OF PHYSICS, 19 ARMII KRAJOWEJ AV., 42-200 CZĘSTOCHOWA, POLAND

a stencil and squeegees bring solder paste to the PCB. Often, solder paste printers have automated systems for inspecting the quantity and surface condition. This may depend on the PCB size. As solder paste printing is time-consuming, a dedicated inspection machine is generally used [9]. Once the solder paste has been confirmed to have been applied correctly, the PCB moves on to the placement of components. The vacuum or gripper nozzles are used to pick components from their packaging. A vision system guarantees the correct positioning, and the components are moved quickly depending on the system's programming. After all components are installed and checked, the PCB assembly goes to the reflow soldering machine. Each step heats the assembly to a predetermined temperature to establish good, reliable solder connections between the components and the PCB. Despite the perceived simplicity of reflow soldering, executing the right reflow profile is vital [10]. This guarantees high-quality solder joints and prevents excessive heat from damaging components or the assembly, particularly for the FPCBs.

Due to the limitations of RPCBs, they are less adapted to modern electronic devices [11]. Consequently, FPCBs were developed as a more favorable option with more flexibility to withstand stress and impact. One of the challenges to RPCBs comes from thermal stress; not only does the substrate consist of gradually different materials with different coefficients of thermal expansion [12]. This differential expansion generates high stress in the materials, which can endanger the integrity of the interconnection joints. This led to many research papers focusing on heat transfer and cooling techniques for RPCBs. The limitations of RPCBs become even more apparent given the challenges, including bending stress, mechanical shock, and joint connections [13]. Thus, alternatives have become preferred, hence the increasing popularity of FPCBs [14].

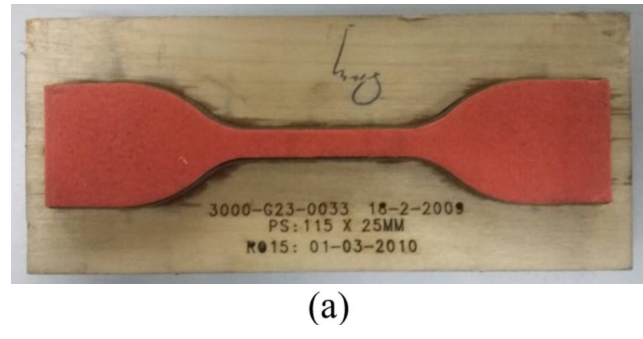
The behavior of fluid flow and thermal factors in FPCBs have been studied in previously published research, especially in the work by Lau et al. [15] on Ball Grid Array (BGA) packaging. However, these studies are also limited because they do not consider the elements mounted on FPCBs, which can influence flexibility and be displaced during reflow soldering. Most known studies have been performed in controlled experimental conditions and do not represent what happens during real reflow soldering conditions. Therefore, experiments were planned to fill this gap and study the temperature effects on FPCBs through the reflow soldering process in real-life situations using a reflow oven. This methodology is more realistic in understanding the behaviors of FPCBs under operating conditions.

2. Methodology

2.1. FPCB Mechanical and Thermal Material Test

In this experiment, a single-sided Flexible Printed Circuit Board (FPCB) was used, comprising a single copper layer and a single polyimide layer, with a total thickness of 0.053 mm. The density of the FPCB was determined using a Shimadzu AU-

W220D Weighing Scale, which has an accuracy of 0.1 mg. The FPCB's mass was measured and divided by volume to calculate its density. A tensile test was performed using an INSTRON 3367 Universal Testing Machine to determine the mechanical properties. This test was conducted to measure the Young's modulus and yield strength of the FPCB. The testing followed the ISO 527-3 standard [16], with a test speed of 0.25 mm/min. Three samples were cut from the FPCB and tested to ensure consistency and reliability (Fig. 1).



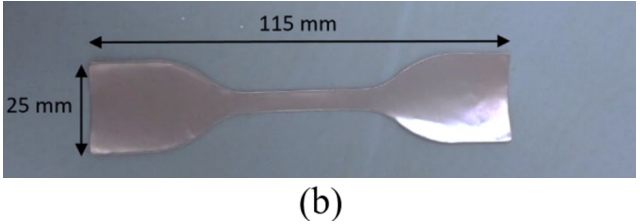


Fig. 1. (a) Die cutter used in sample preparation and (b) FPCB sample with dimensions

The thermal conductivity and specific heat capacity of the Flexible Printed Circuit Board (FPCB) were determined using sophisticated testing techniques to ensure precise measurements. Thermal conductivity measurements were performed using the Hot Disk Thermal Constant Analyzer TPS 2500 S according to the ISO 22207-2 standard [17] developed based on the Transient Plane Source (TPS) principle. It is appropriate for thin film testing. A hot disk sensor was inserted between two FPCB samples during the measurement. The thermal conductivity was measured at 23°C. FPCB samples were cut into a square (5 cm × 5 cm) of sufficient size to fit the 3 cm diameter of the hot disk sensor to test thin films.

The specific heat capacity was determined using a Differential Scanning Calorimeter (DSC) [18]. FPCB, RPCB, and solder paste samples, each weighing approximately 5 to 10 mg, were prepared using a Shimadzu AUW220D analytical balance with an accuracy of 0.1 mg. The samples were then placed in aluminum Tzero pans. The test was conducted with a heating rate of 20°C/min, and the temperature was increased from 30°C to 300°C. Argon gas, set to a 50 mL/min flow rate, was used during the DSC experiment.

To establish a baseline for specific heat capacity, an empty aluminum Tzero pan was first run. A sapphire crimp pan was then used as the standard. Finally, the prepared samples (5-10 mg) were placed in aluminum Tzero pans for measurement. The

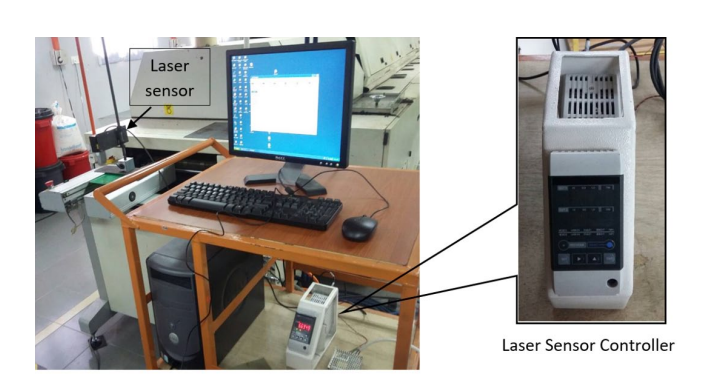
specific heat capacity (C_p) at the desired temperature was calculated using the heat flow versus temperature curves obtained from the baseline, standard, and sample tests. The corresponding equation was applied to compute the specific heat capacity for each sample.

$$C_p = \frac{60 \cdot D_s}{H_r \cdot W_s} \cdot E \tag{1}$$

Where, C_p is a specific heat capacity, D_s is a heat flow difference, H_r is a heating rate, W_s is the weight of the sample and E is a ratio of the heat capacity of standard sapphire and the measured heat capacity.

2.2. Experimental setup for deformation measurement

The deformation measurement experiment utilized a KEY-ENCE LK-G152 laser sensor connected to a controller with an accuracy of 1 µm and a measurement range of 11-18 cm (Fig. 2). The sensor was positioned at the inlet and outlet of a reflow oven to measure deformation caused by warpage before and after the reflow soldering process. The sensor was mounted on a magnetic stand to minimize measurement errors and placed on a stable, non-vibrating surface. The temperature profile and other settings were configured on a computer connected to the BTU Paragon 150 Convection Reflow Oven. The experiment used two temperature profiles, soaking and slumping, to compare their effects on controlling RPCB and FPCB deformation



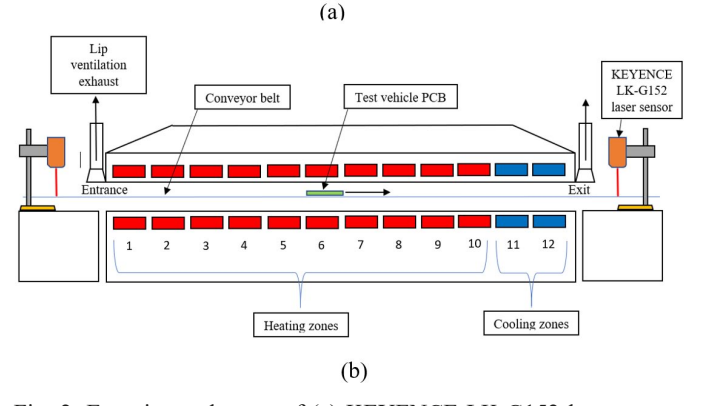


Fig. 2. Experimental setup of (a) KEYENCE LK-G152 laser sensor and (b) schematic diagram of laser sensor setup on the reflow oven

during the reflow soldering. The industrial temperature profiles used are shown in Fig. 3 and Fig. 4. The conveyor speed of the reflow oven was set to 30 inches per minute. The test vehicle was placed on the conveyor at the oven entrance for the experiment. The laser sensor recorded the deformation of the RPCB and FPCB at the outlet, and the quality of the solder joints was inspected and documented.

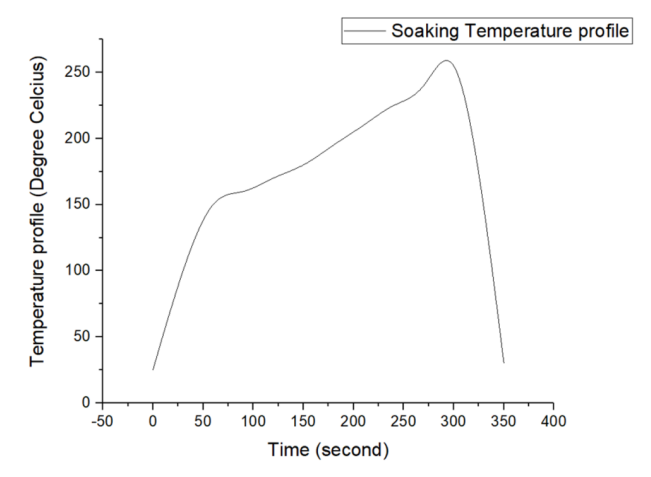


Fig. 3. Soaking temperature profile used in the experiment

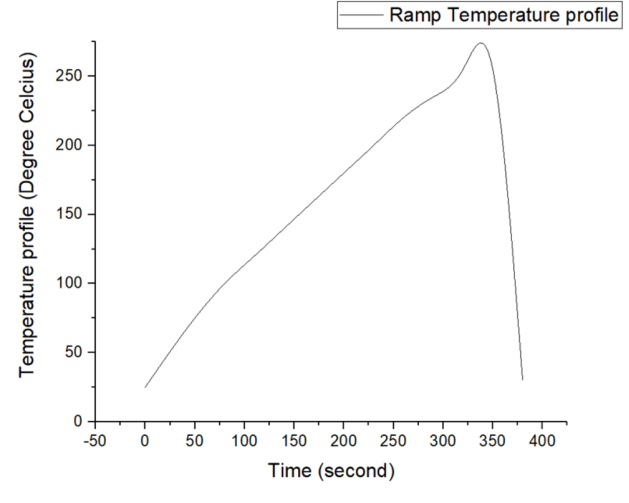


Fig. 4. Ramp temperature profile used in the experiment

3. Results and discussion

3.1. Deformation of FPCB and RPCB during Soaking Temperature Profiles

The deformation behavior of FPCB and RPCB without any attached components was analyzed to understand their material properties and composition when influenced by the temperature profile during the reflow soldering process. Fig. 5 highlights five specific points (A, B, C, D, and E) that were used to compare the initial and final displacements of FPCB and RPCB as they underwent the reflow soldering process. In the soaking temperature profile experiment, Fig. 6 illustrates that the deformation of the FPCB is significantly higher than that of the RPCB at points

A, B, C, D, and E after undergoing the reflow soldering process. The FPCB showed a deformation of up to 1.2634 mm, whereas the RPCB exhibited a much lower deformation of 0.3023 mm. The comparison of the initial and final displacement of FPCB and RPCB is presented in TABLE 1.

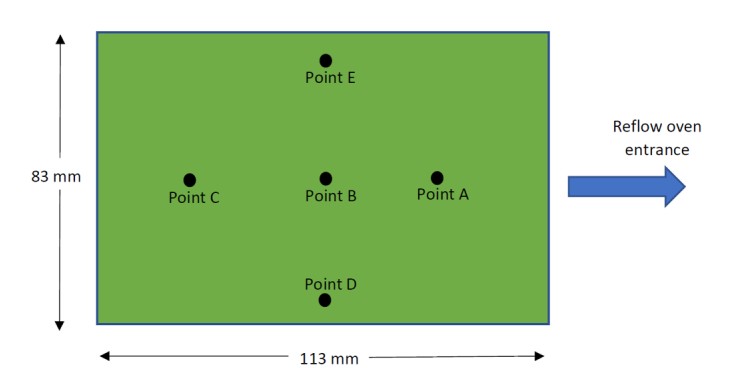


Fig. 5. Five measurement points on FPCB and RPCB test vehicles

The significant deformation in the FPCB can be attributed to the structural property of the FPCB, which consists of thinner material thickness. The thickness of the single copper layer and single polyimide layer in FPCB is only 0.053 mm. During the process, thermal stress is generated simultaneously due to the thermal expansion of the copper layer and the thermal contraction of the polyimide layer. This causes the FPCB to curve into an inverted U shape with the copper layer on top of the polyimide layer. The deformation of the RPCB is thus considerably reduced owing to its substantial thickness and high-quality material properties. Fig. 7 shows the deformation of both FPCB and RPCB.

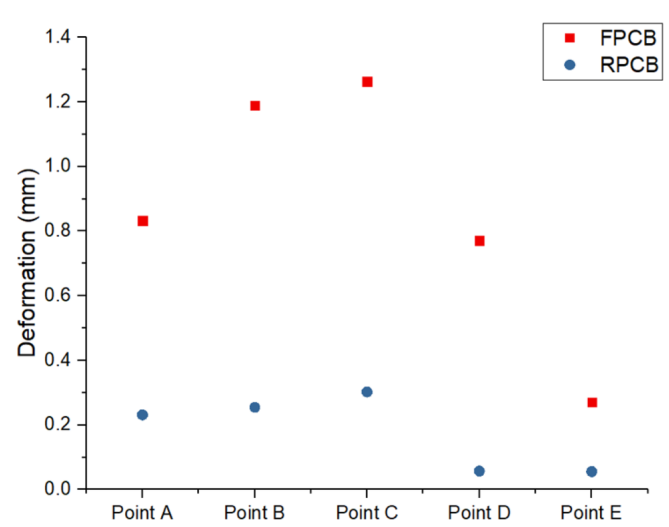


Fig. 6. Deformation of FPCB and RPCB using soaking temperature profile

TABLE 1
Initial and final displacement of FPCB and RPCB for soaking temperature profile

Soaking Temperature Profile										
Point	Displacement of FPCB (mm)		Deflection	Displacement of RPCB (mm)		Deflection				
	Initial	Final	(mm)	Initial	Final	(mm)				
Point A	0.0544	0.8868	0.8324	-0.1789	-0.4103	0.2314				
Point B	0.139	1.3281	1.1891	-0.1595	-0.4142	0.2547				
Point C	0.0627	1.3261	1.2634	-0.0784	-0.3807	0.3023				
Point D	0.1795	0.9507	0.7712	-0.0136	-0.0711	0.0575				
Point E	0.0418	0.3129	0.2711	-0.4273	-0.483	0.0557				

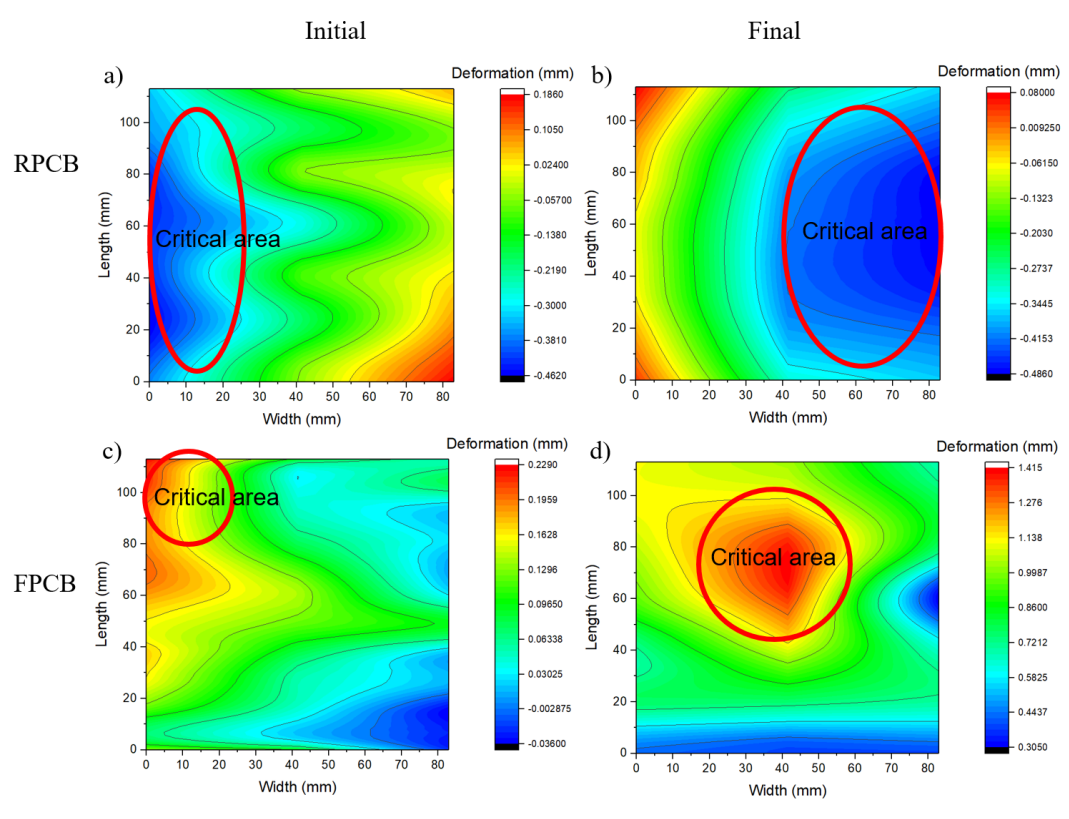


Fig. 7. Contour plot of RPCB and FPCB for soaking temperature profile

According to the Institute for Printed Circuits (IPC) classification [19], Fig. 7(b), the RPCB deformation can be described as bow-type. The RPCB employed in this investigation consists of a solder mask and copper layer with superior thermal stability FR-4 substrate.

According to Fig. 7(d), the critical area with the highest deformation for the FPCB was observed near the center of the sample. Thermal conductivity tests performed with a Hot Disk Thermal Analyzer revealed that the FPCB has a higher thermal conductivity than the RPCB. This characteristic contributes to the increased thermal stress in the FPCB, leading to more significant deformation [20]. While the RPCB's deformation is less critical, it still undergoes some warping due to thermal stress, as indicated in Fig. 7.

3.2. Deformation of FPCB and RPCB during Ramp Temperature Profiles

Under the ramp temperature profile, Fig. 8 demonstrates that the FPCB exhibits significantly greater deformation than the RPCB after the reflow soldering process. The FPCB deforms up to 1.6403 mm, while the RPCB shows a much smaller deformation of only 0.1574 mm. TABLE 2 summarizes the initial and final displacement of FPCB and RPCB for the ramp temperature profile. According to Fig. 9, the final critical deformation area for the RPCB is located at the center of the test vehicle board. In contrast, for the FPCB, it occurs at the corners. Fig. 9(b) indicates that the RPCB deformation can be categorized as

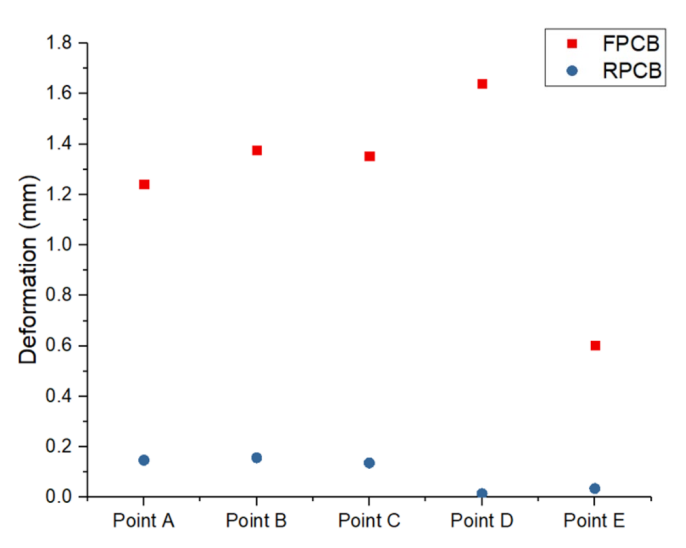


Fig. 8. Deformation of FPCB and RPCB for ramp temperature profile

TABLE 2
Initial and final displacement of FPCB and RPCB for ramp temperature profile

Ramp Temperature Profile										
Point	Displacement of FPCB (mm)		Deflection	Displacement of RPCB (mm)		Deflection				
	Initial	Final	(mm)	Initial	Final	(mm)				
Point A	-0.043	1.1992	1.2422	-0.0566	-0.2043	0.1477				
Point B	0.1128	1.4898	1.377	-0.0699	-0.2273	0.1574				
Point C	0.0441	1.3976	1.3535	-0.0578	-0.1942	0.1364				
Point D	0.0349	1.6752	1.6403	-0.053	-0.0678	0.0148				
Point E	-0.1452	0.4569	0.6021	-0.1608	-0.1957	0.0349				

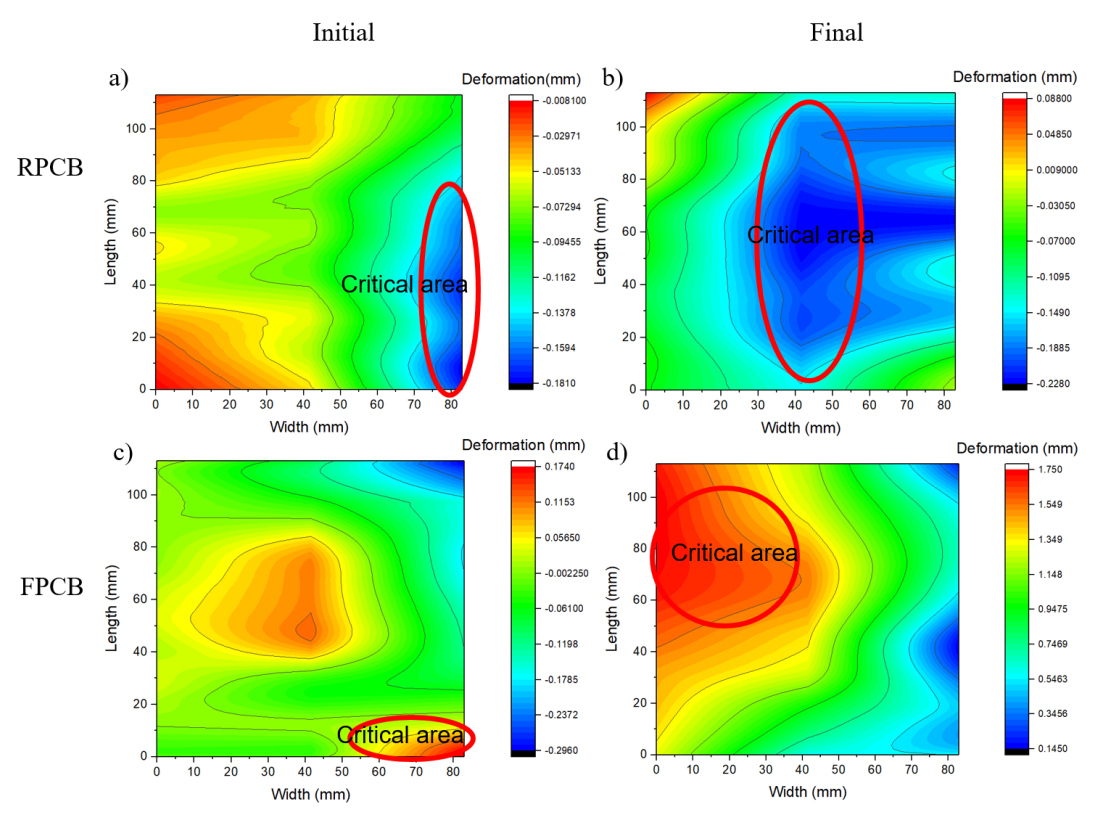


Fig. 9. Contour plot of RPCB and FPCB for ramp temperature profile

a twist type based on the classification by the Institute for Printed Circuits (IPC) [19]. The higher deformation observed in the FPCB compared to the RPCB is attributed mainly to the FPCB's higher thermal conductivity. The thermal conductivity of the FPCB is 40.4% greater than that of the RPCB, leading to increased thermal stress and, consequently, more pronounced deformation in the FPCB.

3.3. Comparison of deformation for Soaking and Ramp Temperature Profiles

As shown in Fig. 10, the deformation of the FPCB under the ramp temperature profile is significantly higher than that under the soaking temperature profile. The maximum deformation for the FPCB in the ramp temperature profile reaches 1.6403 mm, while in the soaking temperature profile, it is 1.2634 mm. On the other hand, Fig. 11 indicates that the deformation of the RPCB is more significant under the soaking temperature profile (0.3023 mm) than the ramp temperature profile (0.1574 mm). The increased deformation of the FPCB under the ramp tempera-

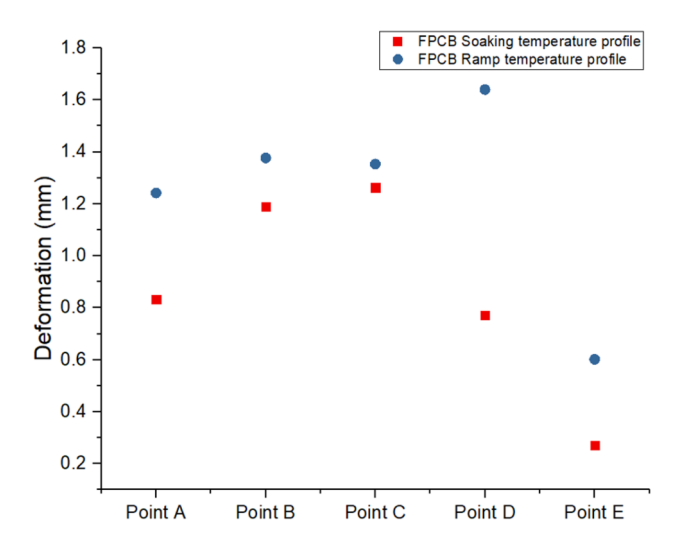


Fig. 10. Deformation of FPCB at soaking and ramp temperature profiles

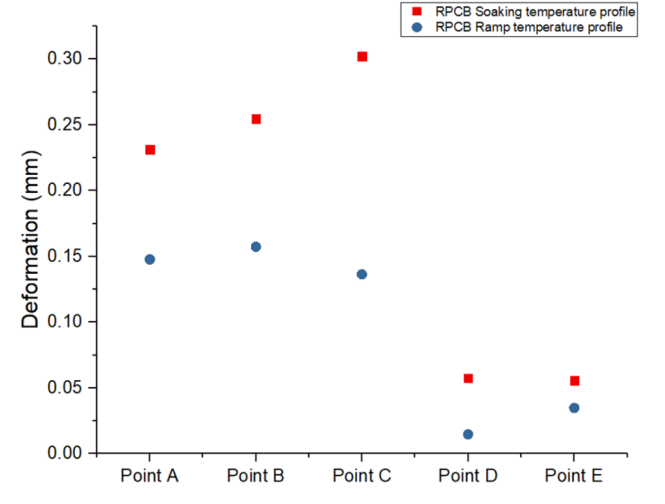


Fig. 11. Deformation of RPCB at soaking and ramp temperature profiles

ture profile is due to the higher thermal stress developed in the FPCB compared to the RPCB. This is attributed to the constant temperature gradient in the ramp temperature profile, as shown in Fig. 4 (Section 2.2). This situation leads to substantial thermal stress in the FPCB. However, the RPCB experiences more significant deformation under the soaking temperature profile. Fig. 3 (Section 2.2) highlights a sudden temperature increase during the preheating stage of the soaking profile, from room temperature to 150°C. This abrupt change creates a thermal shock in the RPCB, as the high thermal gradient causes the materials within the RPCB to expand at varying rates due to their differing thermal expansion coefficients.

4. Conclusion

This experiment was designed to examine the impact of temperature profiles on FPCB and compare it with RPCB to investigate a suitable temperature profile for FPCB in the microelectronics industry. The results reveal that temperature significantly affects the FPCB during reflow soldering, much more than the RPCB, due to differences in thickness and material composition. Properly controlling the reflow oven's temperature profile can help minimize the deflection of FPCB. The findings indicate that the ramp temperature profile results in more deformation (1.6403 mm) for FPCB than the soaking temperature profile (1.2634 mm). This revealed that using the soaking temperature profile for FPCB reduces 23% of deformation compared to the ramp temperature profile. Conversely, for RPCB, the soaking temperature profile (0.3023 mm) causes more deformation than the ramp profile (0.1574 mm). Using the ramp temperature profile for RPCB reduces the deformation by 48% more than the soaking temperature profile. FPCB holds strong market potential due to its flexibility, lightweight nature, and thin size. This study successfully identifies an appropriate temperature profile for minimizing deformation. Since reflow soldering is a reliable process widely used for surface-mounted devices (SMDs) in the microelectronics industry, the insights from this research can support the efficient mass production of FPCB products in industrial applications.

REFERENCES

- [1] T.-N. Tsai, Thermal parameters optimization of a reflow soldering profile in printed circuit board assembly: A comparative study. Appl. Soft Comput. 12 (8), 2601-2613 (2012).
 DOI: https://doi.org/10.1016/j.asoc.2012.03.066
- [2] C.H. Lim, M.Z. Abdullah, I.A. Azid, A. Aziz, Experimental and numerical investigation of flow and thermal effects on flexible printed circuit board. Microelectron. Reliab. 72, 5-17 (2017). DOI: https://doi.org/10.1016/j.microrel.2017.03.022
- [3] A. Petropoulos, D.N. Pagonis, G. Kaltsas, Flexible PCB-MEMS flow sensor. Procedia Eng. 47, 236-239 (2012).
 DOI: https://doi.org/10.1016/j.proeng.2012.09.127

- [4] M. Takamiya et al., Flexible, large-area, and distributed organic electronics closely contacted with skin for healthcare applications. Midwest Symp. Circuits Syst., 829-832 (2014). DOI: https://doi.org/10.1109/MWSCAS.2014.6908543
- [5] A. Antennas, Galaxy S6 to Use FPCB Antennas. 4-5 (2018).
- [6] W.C. Leong, M.Z. Abdullah, C.Y. Khor, Application of flexible printed circuit board (FPCB) in personal computer motherboards: Focusing on mechanical performance. Microelectron. Reliab. 52 (4), 744-756 (2011).
 - DOI: https://doi.org/10.1016/j.microrel.2011.11.003
- [7] D. Koncz-Horváth, G. Gergely, Z. Gácsi, The effect of void formation on the reliability of ED-XRF measurements in lead-free reflow soldering. Arch. Metall. Mater. 60 (2B), 1445-1448 (2015). DOI: https://doi.org/10.1515/amm-2015-0150
- J. Franke, L. Wang, K. Bock, J. Wilde, Electronic module assembly. CIRP Ann. 70 (2), 471-493 (2021).
 DOI: https://doi.org/10.1016/j.cirp.2021.05.005
- [9] S. Qu, Y. Liu, WLCSP Assembly. In: Wafer-Level Chip-Scale Packaging. Springer, New York 2015.
 DOI: https://doi.org/10.1007/978-1-4939-1556-9_9
- [10] G. Cennamo, Surface Mount Reflow Profile Impacts on Reliability. In 2018 Annual Reliability and Maintainability Symposium (RAMS) (pp. 1-6). IEEE.
 DOI: https://doi.org/10.1109/RAM.2018.8463136
- [11] L. Xu, Z. Wang, F. Qiao, Q. Gao, T. Wu, Design and Application of Rigid-Flex Printed Circuit Board in Special Vehicles. In Lecture Notes in Electrical Engineering 2024, 381-389 (2023). DOI: https://doi.org/10.1007/978-981-99-9319-2 44
- [12] S. Heltzel, M.Cauwe, J. Bennett, T. Rohr, Advanced PCB technologies for space and their assessment using up-to-date standards. CEAS Space J. 15 (1), 89-100 (2021). DOI: https://doi.org/10.1007/s12567-021-00404-1

- [13] R. Darveaux, Effect of simulation methodology on solder joint crack growth correlation. Proc. - Electron. Components Technol. Conf., 1048-1058 (2000). DOI: https://doi.org/10.1115/1.1413764
- [14] X. Chen, Y. C. Lin, X. Liu, G.-Q. Lu, Fracture mechanics analysis of the effect of substrate flexibility on solder joint reliability. Eng. Fract. Mech. 72 (17), 2628-2646 (2005). DOI: https://doi.org/10.1016/j.engfracmech.2005.02.008
- [15] C.-S. Lau, M.Z. Abdullah, F.C. Ani, Computational fluid dynamic and thermal analysis for BGA assembly during forced convection reflow soldering process. Solder. Surf. Mt. Technol. 24 (2), 77-91 (2012). DOI: https://doi.org/10.1108/09540911211214659
- [16] D. Pyka, J.J. Słowiński, A. Kurzawa, M. Roszak, M. Stachowicz, M. Kazimierczak, M. Stępczak, D. Grygier, Research on Basic Properties of Polymers for Fused Deposition Modelling Technology. Appl. Sci.-Basel 14 (23), 11151 (2024). DOI: https://doi.org/10.3390/app142311151
- [17] B. Allard, R. Paulus, N. Gros, H. Mezin, D. Gagnon, C. Fradet,
 G. Lambert, Ecofriendly Glue for the Aluminium Electrolysis Pot.
 In Light Metals. 901-910 (2022).
 DOI: https://doi.org/10.1007/978-3-030-92529-1 118
- [18] S. Zhang, Z. Zhang, X. Wang, Y. Gao, X. Liang, Effects of Yttrium (Y) substitution by cerium (ce) on microstructure and corrosion behavior of near-Equiatomicalniy medium-Entropy amorphous alloy ribbons. Arch. Metall. Mater. 67, 637-643 (2022). DOI: https://doi.org/10.24425/amm.2022.137800
- [19] IPC-TM-650. IPC TM 650 2.4.22 Bow and Twist. 2, 1-2.
- [20] C.H. Lim, M.Z. Abdullah, I.A. Azid, C.Y. Khor, A. Aziz, M.H.H. Ishaik, Heat transfer and deformation analysis of flexible printed circuit board under thermal and flow effects. Circuit World. 47 (2), 213-221 (2021).

DOI: https://doi.org/10.1108/CW-02-2020-0016